RESEARCH ARTICLE

Performance Analysis of ACO/DCO-OFDM Hybrid PLC-VLC Receivers With Blanking Non-Linearity

IRVINE MAPFUMO[1], **THOKOZANI SHONGWE**[1], (Senior Member, IEEE),
AND KHALED M. RABIE[2], (Senior Member, IEEE)

[1]Department of Electrical and Electronic Engineering Science, University of Johannesburg, Johannesburg 2006, South Africa
[2]Department of Engineering, Manchester Metropolitan University, M15 6BH Manchester, U.K.

Corresponding author: Irvine Mapfumo (218098465@student.uj.ac.za)

ABSTRACT Blanking non-linearity is broadly used in impulsive noise communication environments due to its efficiency and ease of deployment to mitigate such noise. During the blanking procedure, data samples with impulsive noise are identified and clipped to zero, which removes impulsive noise from the system thereby, improving the system performance. In this regard, this paper investigates the performance of hybrid power line communication-visible light communication (PLC-VLC) systems with blanking nonlinearity. The signal-to-noise (SNR) ratio at the output of the blanking device is deduced using a closed-form analytical expression. The results show that there is good agreement between simulation results and theory if there is a sufficiently large number of orthogonal frequency division multiplexing (OFDM) sub-carriers. In addition, the study also indicates that the blanking method is more effective in curbing impulsive noise in comparison to the clipping technique. According to the threshold optimisation investigations, there exists a worst-case SINR value that minimizes the output SNR at the OFDM receiver after blanking. Furthermore, the findings also revealed that proper blanking threshold selection is essential for obtaining the best performance.

I. INTRODUCTION

Hybrid power line communication - visible light communication (PLC-VLC) systems are implemented through cascading the PLC and VLC technologies, to form a more robust communication system. PLC offers many benefits for building in-home communication networks [1]. It can offer home users broadband internet access, and it has been viewed as a strong contender to offer solutions to spectral scarcity. To enhance the versatility of PLC, it can be cascaded with the VLC technology, and this yields a more reliable and effective hybrid communication system [2], [3], [4], [5]. In such configurations, PLC acts as the primary communication infrastructure, while the VLC acts as the interface with the users [6]. DC-biased optical - orthogonal frequency division multiplexing (DCO-OFDM) and asymmetrically

clipped optical - orthogonal frequency division multiplexing (ACO-OFDM) modulation techniques play an integral part in the successful amalgamation of the PLC and VLC technologies [7], [8]. Both modulation techniques ensure that data from the PLC channel is positive and real-valued, for compatibility with the VLC channel [9]. The first hybrid PLC-VLC system was reported in [10], and the authors used the single carrier binary phase shift keying (SC-BPSK) to integrate the PLC and VLC technologies. The hybrid PLC-VLC systems have since gained a lot of research interest after various studies provided additional findings. The integration of the PLC and VLC technologies presents a challenge when cascaded, as this process introduces noise into the amalgamated system. Impulsive noise is one of the most noticeable types of noise in hybrid PLC-VLC systems. Authors in [11] and [12] presented on the alleviation of impulsive noise in hybrid PLC-VLC systems implemented by DCO-OFDM and ACO-OFDM, respectively.

The associate editor coordinating the review of this manuscript and approving it for publication was Barbara Masini.

One of the primary benefits of OFDM systems is that they are more resistant to impulsive noise in comparison to single carrier networks [13]. This is because in OFDM, impulsive noise is spread across transmitted OFDM subcarriers. However, it was observed that this merit changes into a demerit [14] if the noise energy surpasses a particular level. Thus, in this study, the blanking technique will be used to combat impulsive noise effects due to its ease of use and implementation.

There are several noise cancellation techniques that can be adopted to curb the effects of impulsive noise in hybrid PLC-VLC systems. Two of the most popular techniques are blanking (also known as nulling) and clipping technique [15]. As previously mentioned, the data samples contaminated with impulsive noise are identified via the blanking procedure and clipped to zero, which removes them from the system and enhances system performance. The nulling technique is mathematically represented by (4). On the other hand, the fundamental idea behind the clipping technique is based on detecting the input signal's amplitude in the frequency domain, in the event that the amplitude of the signal exceeds a particular threshold, the signal is then clipped at T, otherwise the signal is let through without interference. The clipping method can be mathematically represented by (5).

A. PRIOR WORKS

Authors in [11] investigated on the inbuilt clipping characteristic of the DCO-OFDM to curb the effects of impulsive noise in a hybrid PLC-VLC system implemented via DCO-OFDM. The results obtained showed that it is important to choose an optimal DC bias value to maximise the performance of the hybrid system. Similar studies were also reported in [12], however, on a hybrid PLC-VLC system implemented by ACO-OFDM. In that study, the researchers utilised the ACO-OFDM's inbuilt nulling feature to combat impulsive noise from the system. Nonetheless, there is no evidence on the analysis of the system performance reported in the paper. It should be noted that numerous studies have examined how blanking non-linearity performs over PLC systems, see [16], [17], and [18]. Similar studies were also reported in [19], [20], and [21], to optimise the performances of OFDM receivers. However, no performance analysis of the ACO/DCO-OFDM hybrid PLC-VLC system with blanking has been studied in the open literature.

B. CONTRIBUTION

In this work, our main focus is to determine the best threshold and optimising the performance of an ACO/DCO-OFDM receiver of a hybrid PLC-VLC system that employs blanking non-linearity. The ACO/DCO-OFDM signal for hybrid PLC-VLC system with a substantial number of subcarriers will be modelled as a real Gaussian process with a half normal distribution. In addition, we will provide detailed theoretical derivations and analysis that will support our simulated results. The contributions of this work can be summarised as follows

- Derive a closed-form expression for the output signal-to-noise ratio (SNR) of the proposed hybrid PLC-VLC system.
- Explore and identify the relationship between different noise parameters and the blanking threshold value.
- Compare the effectiveness of the blanking technique to the clipping technique in mitigating impulsive noise from the proposed system.

C. ORGANIZATION

The remainder of the study is organised as follows. In Section II, the system model is briefly discussed. In Section III, the SNR at the output of blanking non-linearity is derived, and a closed form expression is provided. We then discuss the obtained results in Section IV, and conclude the study in Section V.

II. SYSTEM MODEL

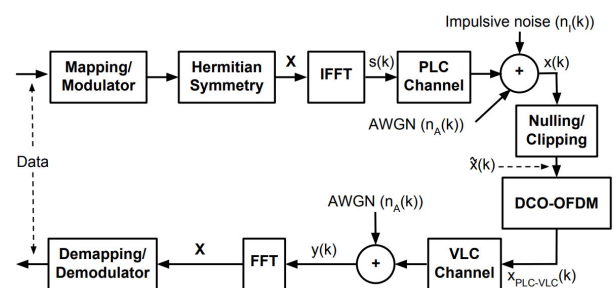We will first give a brief overview of the block diagrams of hybrid systems studied in this work.

FIGURE 1. Hybrid PLC-VLC based on DCO-OFDM [11].

A. HYBRID PLC-VLC BASED ON DCO-OFDM

Fig. 1 shows the block diagram of the hybrid system implemented via DCO-OFDM. Input data is mapped using binary phase shift key (BPSK) and forwarded to the Hermitian symmetry block. The Hermitian block plays a key role in ensuring that the output samples after the inverse fast Fourier transform (IFFT) block are real valued as per requirement of the VLC channel for successful integration with PLC. The signal at the output of the IFFT block is then transmitted to the PLC channel where it is contaminated with impulsive noise and added white Gaussian noise (AWGN). The addition of noise increases the signal amplitude which can alter the signal characteristics. To curb the effects of impulsive noise, the clipping/nulling technique can be used. These noise cancellation techniques will be discussed in detail later on in this paper. A DC bias is added to the clipped/nulled signal so that the samples are positive as required by the VLC channel. The remaining negative samples after DC biasing are then clipped to zero to ensure that all samples are real and positive. At this point, we have a real and positive valued signal which
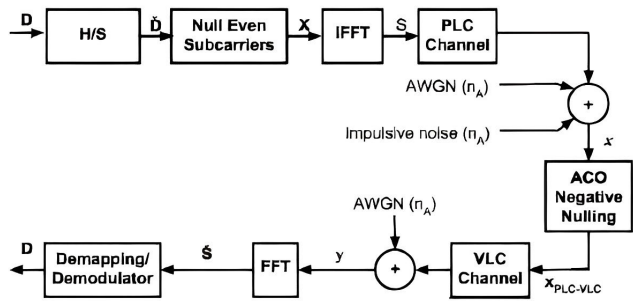
FIGURE 2. Hybrid PLC-VLC based on ACO-OFDM [12].

is compatible with the VLC channel. This signal is forwarded to the VLC channel where it is further corrupted with AWGN before demodulating it to recover the originally sent samples.

B. HYBRID PLC-VLC BASED ON ACO-OFDM

Fig. 2 shows the block diagram of the hybrid system implemented via ACO-OFDM. The signal processing procedure is almost similar to DCO-OFDM except the following. The ACO-OFDM based hybrid system has a block that nulls even subcarriers after the Hermitian symmetry block as part of the ACO-OFDM procedure since it carries useful data on odd subcarriers. To ensure that the PLC signal is real valued and positive, the ACO-OFDM hybrid system employs a ACO negative nulling block that nulls all samples with negative amplitude. This is because in ACO-OFDM, the negative samples are a reflection of the positive samples so no data is lost during this process. Thus, the ACO-OFDM system sends data on real valued and positive odd components.

It is important to note that both the ACO and DCO systems share a similarity in that the samples sent to the VLC channel are real valued and positive. This is because the VLC system requires the samples to be non-negative and real valued for it to be cascaded with the PLC system. Thus in the following analysis, the amplitude of the PLC-VLC signal has a half normal distribution since its samples are real valued. The VLC channel in our system has two types of noise, i.e., thermal noise (modelled as AWGN) and shot noise. Let shot noise and thermal noise be represented by X_{shot} and X_{therm}, respectively. Assuming that the transmitted signal is X, this means that the received signal at the VLC can be represented by $X_{vlc} = X + X_{shot} + X_{therm}$. The transmitted signal the X goes through a VLC channel with a transfer function H, such that $X_{vlc} = HX + X_{shot} + X_{therm}$. If the variance of $X_{therm} > X_{shot}$, then X_{therm} dominates, therefore, the total noise is just modelled as AWGN [24]. It is also imperative to note that the channel gain of an optical propagation link can be null, i.e., when the incident angle > field of view (FOV), a condition when the receiver and a transmitter are not in each other's FOV, see [25].

C. HYBRID PLC-VLC BASED ON ACO/DCO-OFDM

Fig. 3 shows the block diagram for the system model used in this investigation to simplify the analysis of both hybrid

systems. We assume that a BPSK mapped signal S_k undergoes a process to convert it to a real valued signal as part of the ACO/DCO-OFDM signal processing. We have provided a brief overview of the hybrid systems in this work in the previous Section, but the authors in [11] and [12] provide a more detailed explanation on how to attain a real valued signal at the output of an IFFT block for the DCO-OFDM and ACO-OFDM hybrid PLC-VLC systems, respectively. The real valued signal s_k is forwarded to the PLC channel where it is contaminated with impulsive noise i_k, and AWGN g_k. The received signal can be represented as

$$r_k = s_k + g_k + i_k, \tag{1}$$

for a length N-1, where N represent the number of subcarriers. In this study, s_k, g_k and i_k are considered to be independent of one another. In this paper, we assume that the impulsive noise can be characterised as a Bernoulli-Gaussian random process [14], therefore,

$$i_k = g_k b_k, \tag{2}$$

where g_k is the real zero-mean AWGN and b_k is a Bernoulli method, which consists of an independent and uniformly distributed series of ones and zeros, with probability mass function

$$P(b_k) = \begin{cases} p, & \text{if } b_k = 1, \\ 1-p, & \text{otherwise.} \end{cases} \tag{3}$$

The received signal r_k is subjected to the blanking technique at the receiver in order to reduce the energy of impulsive noise. To alleviate the impulsive noise from the system, the following blanking non-linearity

$$y_k = \begin{cases} r_k, & \text{if } |r_k| < T, \\ 0, & \text{otherwise,} \end{cases} \tag{4}$$

or the clipping technique

$$y_k = \begin{cases} r_k, & \text{if } |r_k| < T, \\ T, & \text{otherwise,} \end{cases} \tag{5}$$

is applied to the received signal r_k, where T is the threshold.

(4) and (5) performs noise cancellation on all data samples with large amplitudes assumed to be affected with impulsive noise. Based on knowledge obtained from literature, the required ACO/DCO-OFDM signals could be blanked and distorted if T is too low. However, the ability to reduce impulsive noise is also compromised if T is set too high. As a result, an optimal value of T exists and is obtained from (4). To guarantee that the data delivered to the VLC channel is real valued and positive, the resulting signal, y_k, is sent to a block that clips negative samples to zero.

III. BLANKING NON-LINEARITY SNR OUTPUT

The derivations in this study follow the work in [19], [20], and [21], however, now applied to the ACO/DCO-OFDM Hybrid PLC-VLC receivers. First and foremost, the SNR at the output of the memoryless non-linearity needs to be
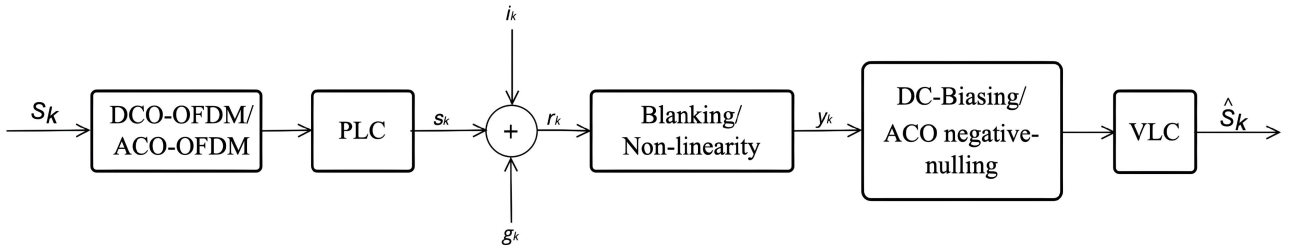
FIGURE 3. The hybrid PLC-VLC system's block diagram with blanking non-linearity.

defined. To achieve this, let us consider the following. To simplify the mathematical annotations in this work, the following definitions are made: $A_s = |s_k|$, $A_g = |g_k|$, $A_r = |r_k|$, and $A_n = |n_k|$, where n_k is the noise after blanking, defined by $n_k = y_k - s_k$.

Under the assumption that there is a sufficiently large number of subcarriers, i.e., $N \to \infty$, the study in this work showed that the ACO/DCO-OFDM signal has a normal Gaussian distribution. As a result, the ACO/DCO-OFDM signal's amplitude can be represented as a real Gaussian process with a half-normal distribution. The ACO/DCO-OFDM signal can be normalised by $\frac{1}{2}E[A_s^2] = \sigma_s^2 = 1$. Let the AWGN noise variance be denoted by $E[A_g^2] = 2\sigma_g^2$ and the impulsive noise variance by $E[|i_k^2|] = 2\sigma_i^2$.

Now, we can consider the SNR at the blanking output which enables us to provide the quantitative characterisation of impulsive noise cancellation from the system, defined as

$$\text{SNR} = \frac{E[|s_k|^2]}{E[|y_k - s_k|^2]} = \frac{2}{E[A_n^2]}. \quad (6)$$

As previously stated, $\{s_k\}$, $\{i_k\}$ and $\{g_k\}$ are all mutually independent white spectrum sequences and (4) is memoryless. Thus, the sequence of n_k has a white spectrum and affects the ACO/DCO-OFDM subcarriers uniformly. Therefore, the performance of the ACO/DCO-OFDM receiver of the proposed system with blanking non-linearity may be described using equation (6).

A. DISTRIBUTION OF NOISE AMPLITUDE AT THE BLANKING NONLINEARITY OUTPUT

The following notations are taken into consideration before we begin the mathematical derivation of the SNR at the output of the blanking nonlinearity: let K be the event of clipping a signal with an amplitude greater that a threshold T, and I as the the event when impulsive noise is present in the system (and $\overline{K}$ and $\overline{I}$ are their compliments, respectively).

Joint event probabilities and conditional probability density functions (PDFs) can be used to express the distribution of the noise amplitude at the output of blanking non-linearity as

$$f(A_n) = P(\overline{K}, \overline{I})f(A_n|\overline{K}, \overline{I}) + P(\overline{K}, I)f(A_n|\overline{K}, I) \\ + P(K, \overline{I})f(A_n|K, \overline{I}) + P(K, I)f(A_n|K, I). \quad (7)$$

Our next objective is to find the conditional probabilities $f(A_n|\overline{K}, \overline{I})$, $f(A_n|\overline{K}, I)$, $f(A_n|K, \overline{I})$, $f(A_n|K, I)$ and probabilities $P(\overline{K}, \overline{I})$, $P(\overline{K}, I)$, $P(K, \overline{I})$, $P(K, I)$. The joint probabilities $P(\overline{K}, \overline{I})$, $P(\overline{K}, I)$, $P(K, \overline{I})$, $P(K, I)$ can be found easily since the amplitude of the received signal A_r always has a half normal distribution. Consider a case where the received samples $\{r_k\}$ are not corrupted with impulsive noise, then A_r has a half normal distribution with parameter $\sigma^2 = 1 + \sigma_g^2$, and the joint probabilities $P(\overline{K}, \overline{I})$ and $P(K, \overline{I})$ can be expressed as

$$P(\overline{K}, \overline{I}) = P(A_r < T|\overline{I})(1 - p)$$
$$= \text{erf}\left(\frac{T}{\sqrt{2(1 + \sigma_g^2)}}\right)(1 - p). \quad (8)$$

where *erf* is the error fuction. If the signal is not clipped,

$$P(K, \overline{I}) = P(A_r > T|\overline{I})(1 - p)$$
$$= \left(1 - \text{erf}\left(\frac{T}{\sqrt{2(1 + \sigma_g^2)}}\right)\right)(1 - p). \quad (9)$$

If the received signal is corrupted with impulsive noise, A_r has a half normal distribution with parameter $\sigma^2 = 1 + \sigma_g^2 + \sigma_i^2$. Thus,

$$P(\overline{K}, I) = P(A_r < T|I)p$$
$$= \text{erf}\left(\frac{T}{\sqrt{2(1 + \sigma_g^2 + \sigma_g^2)}}\right)p. \quad (10)$$

If the signal is not clipped,

$$P(K, I) = P(A_r > T|I)p$$
$$= \left(1 - \text{erf}\left(\frac{T}{\sqrt{2(1 + \sigma_g^2 + \sigma_i^2)}}\right)\right)p. \quad (11)$$

Now, that we have found the expressions for the joint probabilities, the next step is to determine the conditional PDFs. The Bayes' theorem can be used to find the conditional PDFs. Assume a scenario where neither impulsive noise nor clipping event have occurred, i.e, $(\overline{K}, \overline{I})$, then, the only noise source at the blanking output is AWGN. The conditional PDF

of noise can be expressed in terms of Bayes' theorem such that

$$f(A_n|\overline{K},\overline{I}) = \frac{P(A_r < T|A_g,\overline{I})f(A_g)}{P(A_r < T|\overline{I})}. \tag{12}$$

Since A_g has half normal distribution with $\sigma^2 = \sigma_g^2$, therefore, $f(A_g)$ can be represented as

$$f(A_g) = \frac{\sqrt{2}}{\sqrt{\pi\sigma_g^2}}e^{-\frac{A_g}{2\sigma_g^2}}. \tag{13}$$

In the absence of impulsive noise, A_r has a half normal distribution where $\sigma^2 = 1 + \sigma_g^2$. Consequently, $P(A_r < T|\overline{I})$ can be denoted by

$$P(A_r < T|\overline{I}) = \text{erf}\left(\frac{T}{\sqrt{2(1+\sigma_g^2)}}\right). \tag{14}$$

The conditional PDF $f(A_r|A_g, \overline{I})$ has a folded normal distribution with parameter $\mu = A_g$ and $\sigma^2 = 1$. Thus, the corresponding cumulative distribution function in terms of the error function is denoted by

$$P(A_r < T|A_g,\overline{I}) = \frac{1}{2}\left[\text{erf}\left(\frac{T+A_g}{\sqrt{2}}\right) + \text{erf}\left(\frac{T-A_g}{\sqrt{2}}\right)\right]. \tag{15}$$

Substituting (13)−(15) into (12) yields

$$f(A_n|\overline{K},\overline{I}) = \frac{\left[\text{erf}\left(\frac{T+A_g}{\sqrt{2}}\right) + \text{erf}\left(\frac{T-A_g}{\sqrt{2}}\right)\right]\frac{e^{-\frac{A_g}{2\sigma_g^2}}}{\sqrt{2\pi\sigma_g^2}}}{\text{erf}\left(\frac{T}{\sqrt{2(1+\sigma_g^2)}}\right)}. \tag{16}$$

If impulsive noise is present in the received sample r_k, similar analysis is followed. The only contrast in this scenario is that the noise has variance $\sigma_g^2 + \sigma_i^2$. Thus, $f(A_n|\overline{K}, I)$ can be obtained from (16) by substituting $\sigma_g^2 \rightarrow \sigma_g^2 + \sigma_i^2$.

Now a scenario where clipping event has occurred (K) is considered. Then, the noise amplitude A_n is equal to the amplitude of the message signal A_s. That being the case, we need to obtain conditional PDF of A_s following a clipping event. Again, making use of the Bayes' theorem we obtain,

$$f(A_n|K,\overline{I}) = \frac{P(A_r > T|A_s,\overline{I})f(A_s)}{P(A_r > T|\overline{I})}. \tag{17}$$

Recalling that $\sigma_s = 1$, therefore $f(A_s)$ can be written as

$$f(A_s) = \frac{\sqrt{2}}{\sqrt{\pi}}e^{-\frac{A_s}{2}}. \tag{18}$$

Since A_r has a half normal distribution with parameter $\sigma^2 = 1 + \sigma_g^2$, we obtain

$$P(A_r > T|\overline{I}) = 1 - \text{erf}\left(\frac{T}{\sqrt{2(1+\sigma_g^2)}}\right). \tag{19}$$

The conditional PDF $f(A_r|A_s, \overline{I})$ has a folded normal distribution with parameters $\mu = A_s$ and $\sigma = \sigma_g$. Thus, the corresponding conditional probability $P(A_r > T|A_s, \overline{I})$ can be represented as

$$P(A_r > T|A_s,\overline{I})$$
$$= 1 - \frac{1}{2}\left[\text{erf}\left(\frac{T+A_s}{\sqrt{2\sigma_g^2}}\right) + \text{erf}\left(\frac{T-A_s}{\sqrt{2\sigma_g^2}}\right)\right]. \tag{20}$$

Finally, substituting (18)−(20) into (17) yields

$$f(A_n|K,\overline{I}) = \frac{\left[\text{erf}\left(\frac{T+A_s}{\sqrt{2\sigma_g^2}}\right) + \text{erf}\left(\frac{T-A_s}{\sqrt{2\sigma_g^2}}\right)\right]\sqrt{\frac{2}{\pi}}e^{-\frac{A_s}{2}}}{2\left(1 - \text{erf}\left(\frac{T}{\sqrt{2(1+\sigma_g^2)}}\right)\right)}. \tag{21}$$

The analysis is similar when the received samples are corrupted with impulsive noise. $f(A_n|K, I)$ can be obtained from (21) by substituting $\sigma_g^2 \rightarrow \sigma_g^2 + \sigma_i^2$.

B. SNR AT THE BLANKING NONLINEARITY's OUTPUT

After applying blanking, the following step is to determine the average noise energy per sample, which can be calculated as

$$E[A_n^2] = \int_0^\infty A_n^2 f(A_n)\,\mathrm{d}A_n. \tag{22}$$

(22) can be written more conveniently as

$$E[A_n^2] = E(A_n^2|\overline{K},\overline{I})P(\overline{K},\overline{I}) + E(A_n^2|\overline{K}, I)P(\overline{K}, I)$$
$$+ E(A_n^2|K,\overline{I})P(K,\overline{I}) + E(A_n^2|K, I)P(K, I), \tag{23}$$

where $E[A_n^2|K/\overline{K}, I/\overline{I}]$ are conditional expectations defined as

$$E[A_n^2|K/\overline{K}, I/\overline{I}] = \int_0^\infty A_n^2 f(A_n|K/\overline{K}, I/\overline{I})\,\mathrm{d}A_n. \tag{24}$$

Solutions to (24) can be represented in closed-form as

$$E[A_n^2|\overline{K},\overline{I}]$$
$$= \frac{1}{\text{erf}\left(\frac{T}{\sqrt{2(1+\sigma_g^2)}}\right)}$$
$$\times \left[\sigma_g^2\text{erf}\left(\frac{T}{\sqrt{2(1+\sigma_g^2)}}\right) - \frac{T\sigma_g^4 e^{-\frac{T^2}{2(1+\sigma_g^2)}}\sqrt{\frac{2}{\pi}}}{\left(\sqrt{1+\sigma_g^2}\right)^3}\right], \tag{25}$$

and

$$E[A_n^2|K, \bar{I}] = \frac{1}{1 - \mathrm{erf}\left(\frac{T}{\sqrt{1+\sigma_g^2}}\right)} \times \left[1 + \left(\sqrt{1 + \frac{1}{\sigma_g^2}}\right)\right.$$

$$\left. \times \sigma_g \left(\frac{Te^{-\frac{T^2}{2(1+\sigma_g^2)}}\sqrt{\frac{2}{\pi}}}{\left(1+\sigma_g^2\right)^2} - \frac{\mathrm{erf}\left(\frac{T}{\sqrt{2(1+\sigma_g^2)}}\right)}{\sqrt{1+\sigma_g^2}}\right)\right].$$

$$(26)$$

Likewise, $E[A_n^2|\bar{K},I]$ and $E[A_n^2|K,I]$ can be deduced from (25) and (26), respectively, by substituting $\sigma_g^2 \to \sigma_g^2 + \sigma_i^2$. The last step is to substitute (8)−(11), (25) and (26) into (23), which yields (27), as shown at the bottom of the page.

IV. RESULTS AND ANALYSIS

A. THEORETICAL VS SIMULATED BLANKING RESULTS

In this Section, simulation and theoretical results derived in this work are presented. Table 1 shows the simulation parameters used to generate plots in this paper. The impulsive noise probability p and blanking threshold T can be varied to identify their effect on the system performance. It should be noted that we adopted these simulation parameters as they are widely used in many relevant studies, see [20], [21], [22], and [23]. The system performance was found to work well with a large number of subcarriers N hence it is set high in this paper. From literature review, a communication system with SNR of 20–25 dB is more recommended for data and voice applications. In addition, an SNR of 40 dB is deemed excellent for Wi-Fi signal and delivers better network services. Hence the choice to use above SNR values for simulation in some of the plots presented in this paper.

The output SNR vs threshold values are plotted together, for a large number of subcarriers ($N = 10^7$). For all figures presented in this work unless stated otherwise, $\sigma_g^2 = 10^{-2.5}$ (where SNR is defined as $1/\sigma_g^2$), $\sigma_i^2 = 10^{1.5}$ and $N = 10^7$. Fig. 4 shows the performance of an ACO/DCO-OFDM based hybrid PLC-VLC system at $p = 0.01$ and $p = 0.05$. It can be

seen from Fig. 4 that the simulation results are in perfect agreement with the theoretical results obtained in (27).

It can be observed from Fig. 4 that at low T, the output SNR is low. As the threshold is increased, the output SNR increases and reaches a peak. Further increase of the threshold beyond the peak results in system degradation leading to error floor. An explanation to this behaviour is that, at low T, a large part of the ACO/DCO-OFDM signal is replaced with zeros hence the output SNR is low. This is because a low T has an extremely low amplitude hence it fails to differentiate between the clean and impulsive noise corrupted signals. In contrast, if T is too high, impulsive noise is let into the system which degrades the system performance. Thus, there exists an optimal threshold T_{opt}, that maximises the output SNR, $\mathrm{SNR_{max}}$, at the output of the blanking non-linearity. From Fig. 4, for $p = 0.01$, $T_{opt} = 3.5$, and $\mathrm{SNR_{max}} = 17.39$ dB.
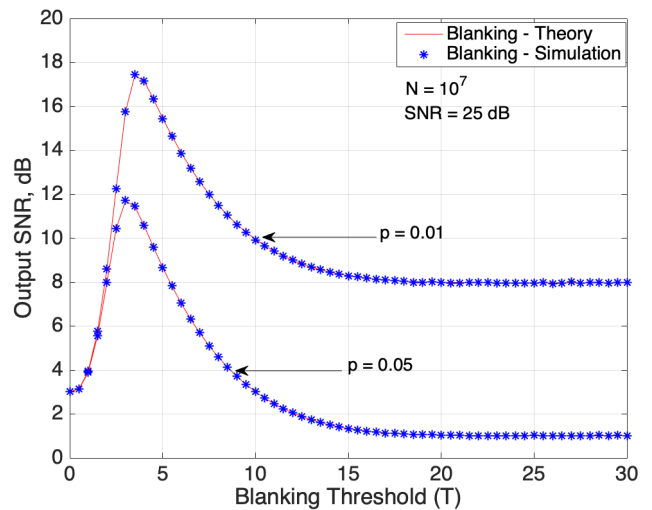

FIGURE 4. Hybrid PLC-VLC system performance at $p = 0.01$ and $p = 0.05$.

At $p = 0.05$, it can be observed that the simulation results are in perfect agreement with the theoretical results obtained in (27). Similar to the performance observed when $p = 0.01$,

$$E[A_n^2] = (1-p) \times \left[1 + \left(\sqrt{1 + \frac{1}{\sigma_g^2}}\right) \times \sigma_g \left(\frac{Te^{-\frac{T^2}{2(1+\sigma_g^2)}}\sqrt{\frac{2}{\pi}}}{\left(1+\sigma_g^2\right)^2} - \frac{\mathrm{erf}\left(\frac{T}{\sqrt{2(1+\sigma_g^2)}}\right)}{\sqrt{1+\sigma_g^2}}\right) - \frac{T\sigma_g^4\sqrt{\frac{2}{\pi}}e^{-\frac{T^2}{2(1+\sigma_g^2)}}}{\left(\sqrt{1+\sigma_g^2}\right)^3} + \sigma_g\mathrm{erf}\left(\frac{T}{\sqrt{2(1+\sigma_g^2)}}\right)\right]$$

$$+ p \times \left[1 + \sqrt{1 + \frac{1}{\sigma_g^2 + \sigma_i^2}} \times \left(\frac{Te^{-\frac{T^2}{2(1+\sigma_g^2+\sigma_i^2)}}\sqrt{\frac{2(\sigma_g^2+\sigma_i^2)}{\pi}}}{\left(1+\sigma_g^2+\sigma_i^2\right)^2} - \sqrt{\frac{\sigma_g^2+\sigma_i^2}{1+\sigma_g^2+\sigma_i^2}}\mathrm{erf}\left(\frac{T}{\sqrt{2(1+\sigma_g^2+\sigma_i^2)}}\right)\right)\right.$$

$$\left. - \frac{T(\sigma_g^2+\sigma_i^2)^2\sqrt{\frac{2}{\pi}}e^{-\frac{T^2}{2(1+\sigma_g^2+\sigma_i^2)}}}{\left(\sqrt{1+\sigma_g^2+\sigma_i^2}\right)^3} + \sqrt{\sigma_g^2+\sigma_i^2}\mathrm{erf}\left(\frac{T}{\sqrt{2(1+\sigma_g^2+\sigma_i^2)}}\right)\right].$$

$$(27)$$

TABLE 1. Simulation parameters.

Symbol	Quantity
p	Impulsive noise probability
σ_i^2	Impulsive noise variance
σ_g^2	Gaussian noise variance
T	Blanking/Clipping Threshold
T_{opt}	Blanking/Clipping Threshold
N	Number of subcarriers

it can be noticed that there exist an optimum threshold T_{opt} that maximises the SNR at the output of the blanking non-linearity. When $p = 0.05$, $T_{opt} = 3$ and $\text{SNR}_{max} = 11.69$ dB.

Results obtained from Fig. 4 for both $p = 0.01$ and $p = 0.05$ share some common traits. It can be observed that there is an optimum threshold that maximises SNR at the output of the blanking non-linearity for every p. SNR_{max} is achieved when the important part of the data is retained as much as possible after the blanking non-linearity. In addition, it is noted that as $T \to \infty$, the SNR at the output of the blanking non-linearity approaches a fixed value, a region called the error floor region. In this region, no blanking operation is performed since T is too high to detect impulsive noise. For both impulsive noise scenarios, the error floor region starts approximately at $T = 18.5$. When $p = 0.01$, the corresponding SNR at the error floor region is $\text{SNR}_{erf} = 8$ dB while at $p = 0.05$, $\text{SNR}_{erf} = 1.22$ dB.

A close look at Fig. 4 also shows the impact of impulsive noise probability value p on the system's performance. Increasing impulsive noise probability from $p = 0.01$ to $p = 0.05$ degrades the performance of the system. The output SNR at the output of the blanking non-linearity plumets as p is increased. At $p = 0.01$, $\text{SNR}_{max} = 17.39$ dB while at $p = 0.05$, $\text{SNR}_{max} = 11.69$ dB, which is 5.7 dB difference.
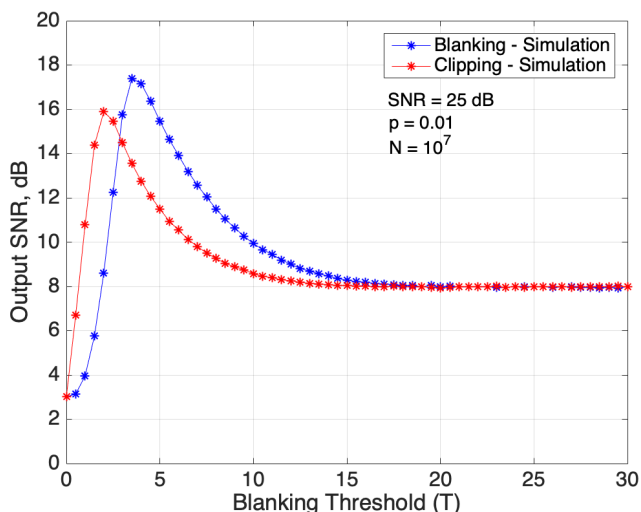

FIGURE 5. Blanking vs clipping at $p = 0.01$.

B. BLANKING VS CLIPPING TECHNIQUE

Fig. 5 shows a comparison in performance between blanking and clipping technique when applied to the proposed system

at $p = 0.01$. It is evident that the blanking technique is more effective offering the optimum SNR because it replaces the corrupted samples completely with zeros, therefore, eliminating all the impulsive noise from the system. This can be witnessed in Fig. 5, the blanking technique offers the highest output SNR of 17.41 dB at its optimum blanking threshold, whereas, the clipping technique has lower output SNR of 15.89 dB at its optimum clipping threshold. Table 2 shows the summary on the performance of hybrid system under different channel scenarios where we classify the noise level into three categories, namely, low, medium, and high with some descriptions. The tabulated results were obtained by varying the impulsive noise level injected into the transmission channel. It is evident from the results presented in Table 2 that if there is a lot of impulsive noise in the channel the system performance is low as indicated by a low SNR. In contrary, if the impulsive noise present in the channel is low, a high SNR can be achieved, which is ideal for data transmission. The results in Table 2 are constant across all impulsive noise levels, indicating that the blanking technique is the most preferable way to reduce impulsive noise to reach higher SNR values.

C. THRESHOLD OPTIMISATION

The performance of the hybrid system is dependent on T, as seen from the results from the preceding section. If the clipping threshold T is set too high, it allows impulsive noise to pass through, as a consequence, degrading the system performance. In contrary, if T is set too low, we risk replacing a considerable amount of of the useful signal by zeros, thereby notably decreasing the output SNR. This implies that an ideal threshold value, T_{opt}, exists that maximizes output SNR. T_{opt} can be found by determining the solution to

$$\frac{\delta E[A_n^2]}{\delta T} = 0. \tag{28}$$

Equation (28) has a single real solution ($T > 0$) and is preferably expressed in closed-form (see [18] for details)

$$T_{opt} = \left(\ln \left(\frac{p-1}{p} \frac{1-\sigma_g^2}{1-\sigma_g^2-\sigma_i^2} \left[\frac{1+\sigma_g^2+\sigma_i^2}{1+\sigma_g^2} \right]^{3/2} \right) \right.$$
$$\left. \times \sqrt{\frac{2(1+\sigma_g^2)(1+\sigma_g^2+\sigma_i^2)}{\sigma_i^2}} \right). \tag{29}$$

A closer look to equation (29) can tell us the following. As $\sigma_g^2 + \sigma_i^2 \to \infty$, the optimal threshold approaches infinity. In addition, if $\sigma_g^2 + \sigma_i^2 > 1$, then a real solution to equation (28) does not exist. This result is in line with the intuitive reasoning that blanking nonlinearity does not enhance system performance if the variance of impulsive noise is less than the variance of the signal. Fig. 6 presents the numerical results from (28) plotted vs the SINR.

T_{opt} in equation (29) can be substituted into (27) to obtain the output SNR at optimal threshold. The corresponding output SNR can be plotted vs SINR as shown in Fig. 6. SINR

TABLE 2. Channel scenarios.

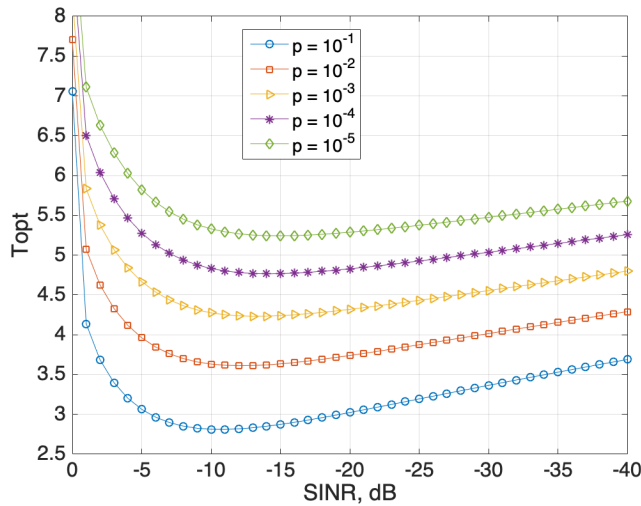| Impulsive noise probability	SNR at Peak (Blanking)	SNR at Peak (Clipping)
Low ($p = 0.001$)	24.18 dB	22.83 dB
Medium ($p = 0.01$)	17.37 dB	15.88 dB
High ($p = 0.1$)	9.24 dB	8.29 dB

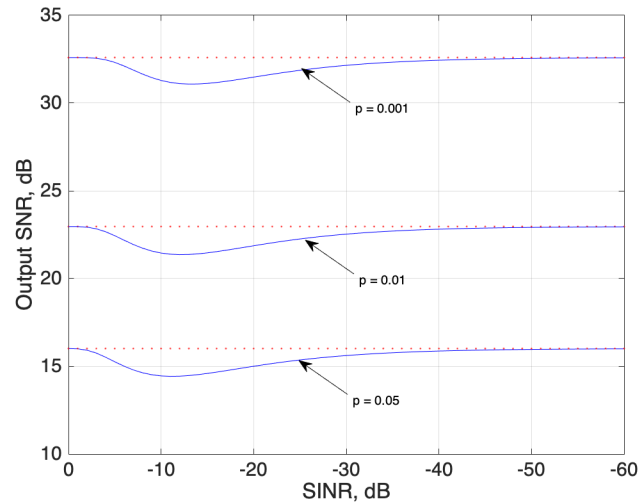**FIGURE 6.** Optimal threshold (T_{opt}) vs signal SINR (at SNR = 40 dB).

FIGURE 7. Maximum achievable SNR at the output of blanking nonlinearity versus SINR at SNR = 40 dB. The dashed line is the estimation.

can be expressed as

$$SINR = \frac{E[|s_k^2|]}{E[|i_k^2|]} = \frac{1}{\sigma_i^2}. \tag{30}$$

Looking at Fig. 7, it can be observed that for every probability p chosen, there lies a worst case SINR that can minimise the output SNR defined in (6). As the SINR $\to \infty$, the output SNR is maximised, which is equivalent to transmission without impulsive noise. In contrary, as SINR approaches zero, while applying an optimal threshold to the signal, all the data samples without impulsive noise impulsive noise remain unclipped. As SINR approaches infinity, the amplitude of any data samples affected by impulsive noise is significantly higher than the average amplitude of the useable signal samples, this means that the straightforward threshold detection approach can be utilised to detect impulsive noise without errors. Thus, we can approximate the total noise energy by

$$\lim_{\substack{\sigma_i^2 \to \infty \\ T = T_{opt}}} E[|A_n^2|] = \sigma_g(1 - p) + p. \tag{31}$$

It should be noted that approximation (31) is only reliable for very low SINR values, which are hardly seen in practical applications. One can see from Fig. 7 that from -2 dB, the actual receiver's performance starts to deteriorate and is at its worst at approximately -11 dB in comparison to the predicted approximation (31). For the cases shown in Fig. 7, the output SNR can vary by up to 2 dB when compared to the scenario when the SINR is nearing zero.

V. CONCLUSION

In this paper, we have derived an expression of the SNR output of the blanking non-linearity and also provided analysis of the performance of the considered hybrid PLC-VLC system. It was observed that for such a system, there exists an optimal threshold that maximises the SNR output for every p. In addition, as $T \to \infty$, the systems presents an error floor where the noise in the system can no longer be detected and cancelled. The obtained simulation results are in agreement with the derived closed form expression. Therefore, the proposed analysis provides an excellent prediction to the output SNR. In addition, the comparative study between the blanking and clipping technique showed that the blanking method is more viable than its competitor based on the results obtained from Fig. 5. The threshold optimisation studies showed that there exist a worst case SINR value that minimises the output SNR at the OFDM receiver when the blanking method is applied. This was caused by errors encountered when detecting signal samples affected by impulsive noise.

REFERENCES

[1] C. Cano, A. Pittolo, D. Malone, L. Lampe, A. M. Tonello, and A. G. Dabak, "State of the art in power line communications: From the applications to the medium," *IEEE J. Sel. Areas Commun.*, vol. 34, no. 7, pp. 1935–1952, Jul. 2016.

[2] H. Ma, L. Lampe, and S. Hranilovic, "Hybrid visible light and power line communication for indoor multiuser downlink," *IEEE/OSA J. Opt. Commun. Netw.*, vol. 9, no. 8, pp. 635–647, Aug. 2017.

[3] H. Ma, L. Lampe, and S. Hranilovic, "Coordinated broadcasting for multiuser indoor visible light communication systems," *IEEE Trans. Commun.*, vol. 63, no. 9, pp. 3313–3324, Sep. 2015.

[4] M. Kashef, M. Abdallah, K. Qaraqe, H. Haas, and M. Uysal, "Coordinated interference management for visible light communication systems," *J. Opt. Commun. Netw.*, vol. 7, no. 11, p. 1098, Nov. 2015.

[5] A. Ndjiongue, T. Shongwe, H. C. Ferreira, T. M. N. Ngatched, and A. J. H. Vinck, "Cascaded PLC-VLC channel using OFDM and CSK techniques," in *Proc. IEEE Global Commun. Conf. (GLOBECOM)*, San Diego, CA, USA, Dec. 2015, pp. 1–6.

[6] T. Komine, S. Haruyama, and M. Nakagawa, "Performance evaluation of narrowband OFDM on integrated system of power line communication and visible light wireless communication," in *Proc. 1st Int. Symp. Wireless Pervasive Comput.*, Mar. 2006, pp. 6–10.

[7] I. Mapfumo, T. Shongwe, and K. Rabie, "Analysis of the perfect nulling technique in FFT hybrid PLC-VLC system based on ACO-OFDM in impulsive noise," in *Proc. Int. Wireless Commun. Mobile Comput. (IWCMC)*, May 2022, pp. 1183–1188.

[8] I. Mapfumo and T. Shongwe, "Performance comparison of FFT and DHT hybrid PLC-VLC systems based on DCO-OFDM in impulsive noise," in *Proc. 30th Int. Conf. Radioelektronika (RADIOELEKTRONIKA)*, Apr. 2020, pp. 1–6.

[9] H. Ma, L. Lampe, and S. Hranilovic, "Integration of indoor visible light and power line communication systems," in *Proc. IEEE 17th Int. Symp. Power Line Commun. Appl.*, Mar. 2013, pp. 291–296.

[10] T. Komine and M. Nakagawa, "Integrated system of white LED visible-light communication and power-line communication," in *Proc. 13th IEEE Int. Symp. Pers., Indoor Mobile Radio Commun.*, Sep. 2002, pp. 1762–1766.

[11] M. D. Kubjana, A. R. Ndjiongue, and T. Shongwe, "Impulsive noise evaluation on PLC-VLC based on DCO-OFDM," in *Proc. 11th Int. Symp. Commun. Syst., Netw. Digit. Signal Process. (CSNDSP)*, Jul. 2018, pp. 1–6.

[12] M. D. Kubjana, T. Shongwe, and A. R. Ndjiongue, "Hybrid PLC-VLC based on ACO-OFDM," in *Proc. Int. Conf. Intell. Innov. Comput. Appl. (ICONIC)*, Dec. 2018, pp. 1–5.

[13] S. D. Dissanayake and J. Armstrong, "Comparison of ACO-OFDM, DCO-OFDM and ADO-OFDM in IM/DD systems," *J. Lightw. Technol.*, vol. 31, no. 7, pp. 1063–1072, Apr. 1, 2013.

[14] M. Ghosh, "Analysis of the effect of impulse noise on multicarrier and single carrier QAM systems," *IEEE Trans. Commun.*, vol. 44, no. 2, pp. 145–147, Feb. 1996.

[15] A. G. Bolaji and T. Shongwe, "Investigation on ways to mitigate the combination of impulsive noise and narrowband noise within a single channel," in *Proc. Int. Conf. Adv. Big Data, Comput. Data Commun. Syst. (icABCD)*, Aug. 2018, pp. 1–5.

[16] F. Ayaz, K. Rabie, and B. Adebisi, "Analysis of optimized threshold with SLM based blanking non-linearity for impulsive noise reduction in power line communication systems," in *Proc. 11th Int. Symp. Commun. Syst., Netw. Digit. Signal Process. (CSNDSP)*, Jul. 2018, pp. 1–6.

[17] F. H. Juwono, Q. Guo, D. Huang, Y. Chen, L. Xu, and K. P. Wong, "On the performance of blanking nonlinearity in real-valued OFDM-based PLC," *IEEE Trans. Smart Grid*, vol. 9, no. 1, pp. 449–457, Jan. 2018.

[18] C.-H. Yih, "Iterative interference cancellation for OFDM signals with blanking nonlinearity in impulsive noise channels," *IEEE Signal Process. Lett.*, vol. 19, no. 3, pp. 147–150, Mar. 2012.

[19] S. V. Zhidkov, "Analysis and comparison of several simple impulsive noise mitigation schemes for OFDM receivers," *IEEE Trans. Commun.*, vol. 56, no. 1, pp. 5–9, Jan. 2008.

[20] S. V. Zhidkov, "On the analysis of OFDM receiver with blanking nonlinearity in impulsive noise channels," in *Proc. Int. Symp. Intell. Signal Process. Commun. Syst. (ISPACS)*, Nov. 2004, pp. 492–496.

[21] S. V. Zhidkov, "Performance analysis and optimization of OFDM receiver with blanking nonlinearity in impulsive noise environment," *IEEE Trans. Veh. Technol.*, vol. 55, no. 1, pp. 234–242, Jan. 2006.

[22] I. Mapfumo and T. Shongwe, "A comparison of FFT and DHT hybrid PLC-VLC systems based on ACO-OFDM in impulsive noise," in *Proc. 30th Int. Conf. Radioelektronika (RADIOELEKTRONIKA)*, Apr. 2020, pp. 1–7.

[23] T. Shongwe, A. J. Han Vinck, and H. C. Ferreira, "The effects of periodic impulsive noise on OFDM," in *Proc. IEEE Int. Symp. Power Line Commun. Appl. (ISPLC)*, Mar. 2015, pp. 189–194.

[24] P. F. Mmbaga, J. Thompson, and H. Haas, "Performance analysis of indoor diffuse VLC MIMO channels using angular diversity detectors," *J. Lightw. Technol.*, vol. 34, no. 4, pp. 1254–1266, Feb. 15, 2016.

[25] T. Fath and H. Haas, "Performance comparison of MIMO techniques for optical wireless communications in indoor environments," *IEEE Trans. Commun.*, vol. 61, no. 2, pp. 733–742, Feb. 2013.

IRVINE MAPFUMO received the B.Eng. degree in electrical and electronics engineering from the University of Swaziland, in 2017, and the M.Eng. degree in electrical and electronics engineering from the University of Johannesburg, South Africa, in 2021, where he is currently pursuing the Ph.D. degree in telecommunications with the Department of Electrical and Electronics Engineering. His research interests include power line communication (PLC), visible light communication (VLC), and signal processing. He was a recipient of the 2019/2020 University of Johannesburg Global Excellence Stature (GES) Award, which was awarded to him to carry out his master's research with the University of Johannesburg, where he was also awarded the University of Johannesburg Special University Research Committee (URC) Scholarship, in 2021 and 2023, which was awarded to him to carry out his Ph.D. studies. In 2017, he received the Best Student Award of Electronics Engineering from the University of Swaziland.

THOKOZANI SHONGWE (Senior Member, IEEE) received the B.Eng. degree in electronic engineering from the University of Swaziland, Swaziland, in 2004, the M.Eng. degree in telecommunications engineering from the University of the Witwatersrand, South Africa, in 2006, and the D.Eng. degree from the University of Johannesburg, South Africa, in 2014. He is currently an Associate Professor with the Department of Electrical and Electronic Engineering Technology, University of Johannesburg. His research interests include digital communications and error correcting coding, power-line communications, cognitive radio, smart grids, visible light communications, machine learning, and artificial intelligence. He was a recipient of the 2014 University of Johannesburg Global Excellence Stature (GES) Award, which was awarded to him to carry out his postdoctoral research with the University of Johannesburg. In 2016, he was a recipient of the TWAS-DFG Cooperation Visits Programme funding to do research in Germany. Other awards that he has received in the past are: the Postgraduate Merit Award Scholarship to pursue his master's degree from the University of the Witwatersrand, in 2005, which is awarded on a merit basis. In 2012, he (and his coauthors) received an award of the Best Student Paper at the IEEE ISPLC 2012 (power line communications conference), Beijing, China.

KHALED M. RABIE (Senior Member, IEEE) received the M.Sc. and Ph.D. degrees in electrical and electronic engineering from the University of Manchester, in 2011 and 2015, respectively. He is currently a Reader with the Department of Engineering, Manchester Metropolitan University (MMU), U.K. He has a part of several large-scale industrial projects and has published more than 200 journals and conference articles (mostly IEEE). His current research interests include designing and developing next-generation wireless communication systems. He is also a fellow of the U.K. Higher Education Academy (FHEA). He regularly serves on the Technical Program Committee (TPC) for several major IEEE conferences, such as GLOBECOM, ICC, and VTC. He has received many awards over the past few years in recognition of his research contributions, including the best paper awards at the 2021 IEEE CITS and the 2015 IEEE ISPLC and the IEEE Access Editor of the month award, in August 2019. He is currently serving as an Editor for IEEE COMMUNICATIONS LETTERS, an Editor for *IEEE Internet of Things Magazine*, an Associate Editor for IEEE ACCESS, and an Executive Editor for the *Transactions on Emerging Telecommunications Technologies* (Wiley). He has guest-edited many special issues in journals, including *IEEE Wireless Communications Magazine*, in 2021, *Electronics*, in 2021, *Sensors*, in 2020, and IEEE ACCESS, in 2019.

● ● ●